

**Electronic Supplementary Material****Facile synthesis of Ru-incorporated NiFe–MOF nanosheet heterostructures as an efficient bifunctional electrocatalyst**

Fangqing Zou<sup>1,2</sup>, Ye Xiao<sup>2</sup>, Xianshu Qiao<sup>1</sup>, Chuanjin Tian (✉)<sup>1</sup>,  
and Chang-An Wang (✉)<sup>2</sup>

1 Jiangxi Key Laboratory of Advanced Ceramic Materials, School of Materials Science and Engineering, Jingdezhen Ceramic University, Jingdezhen 333403, China

2 State Key Laboratory of New Ceramic Materials, School of Materials Science and Engineering, Tsinghua University, Beijing 100084, China

E-mails: tiancj11@139.com (C.T.), wangca@mail.tsinghua.edu.cn (C.W.)

## 1 Characterization

The X-ray diffraction (XRD) characterization of samples was qualitatively analyzed using a Bruker-D8 Advanced X-ray diffractometer from Germany. Cu K $\alpha$  was used as the target material (the wavelength of X-ray was 0.15418 nm), the working voltage was 40 kV, the working current was 60 mA, and the scanning range was from 10° to 80°. The microscopic morphology of the samples was observed by a MERLIN Compact, Zeiss, Germany scanning electron microscope (SEM) and a LIBRA200, Zeiss, Germany transmission electron microscope (TEM). The elemental composition and valence states of the samples were analyzed by an ESCALAB 250 XI (USA) X-ray photoelectron spectrometer (XPS). The Ru element in the catalyst was quantitatively analyzed using an Agilent 5110 (OES) inductively coupled plasma-atomic emission spectrometer (ICP-OES) made in the United States.

## 2 Preparation of commercial catalysts and electrochemical measurements

Disperse 5 mg of RuO<sub>2</sub> into 1 mL of the mixed solution composed of 0.2 mL of deionized water, 0.77 mL of ethanol, and 0.03 mL of Nafion. Subsequently, ultrasonically disperse the mixture for 1 h to achieve a uniformly dispersed suspension. Using a dropper, apply the suspension onto the nickel foam (with a size of 1 cm × 2 cm), and then dry it in air at 50 °C for 8 h to obtain RuO<sub>2</sub>/NF. The synthesis process was similar to that of RuO<sub>2</sub>@NF, except that RuO<sub>2</sub> was replaced by 20 wt.% Pt/C.

In the three-electrode system, the catalyst served as the working electrode, while a carbon rod was employed as the counter electrode, and the mercury–mercuric oxide was used as the reference electrode. All the tests were carried out in 1 mol·L<sup>-1</sup> KOH electrolyte using a CHI 660E electrochemical workstation from Shanghai Chenhua. Both the OER and HER were evaluated at a constant temperature of 27 °C. In this work, all the potentials were converted from the measured potentials *vs.* Hg/HgO to the reversible hydrogen electrode (RHE) according to the Nernst equation ( $E_{\text{RHE}} = E_{\text{Hg/HgO}} + 0.059 \times \text{pH} + 0.098$ ), and all the currents were converted to current densities.

Additionally, Both the OER and HER curves were corrected by  $iR$  for accuracy.

The polarization curves were evaluated using linear sweep voltammetry (LSV) with a scanning rate of  $5 \text{ mV}\cdot\text{s}^{-1}$ . The solution resistance and charge transfer resistance were tested by electrochemical impedance spectroscopy (EIS). The test frequency range was from 0.01 Hz to 1000 kHz, and the amplitude was 5 mV. In the non-Faradaic region, the electrochemical active surface area (ECSA) of the catalyst was evaluated by the double-layer capacitance ( $C_{dl}$ ). The  $C_{dl}$  values of the catalyst were obtained through cyclic voltammetry (CV) at scanning rates of 20, 40, 60, 80, 100, and  $120 \text{ mV}\cdot\text{s}^{-1}$ . Additionally, the stability of the catalyst was examined through chronopotentiometry at a current density of  $10 \text{ mA}\cdot\text{cm}^{-2}$ .

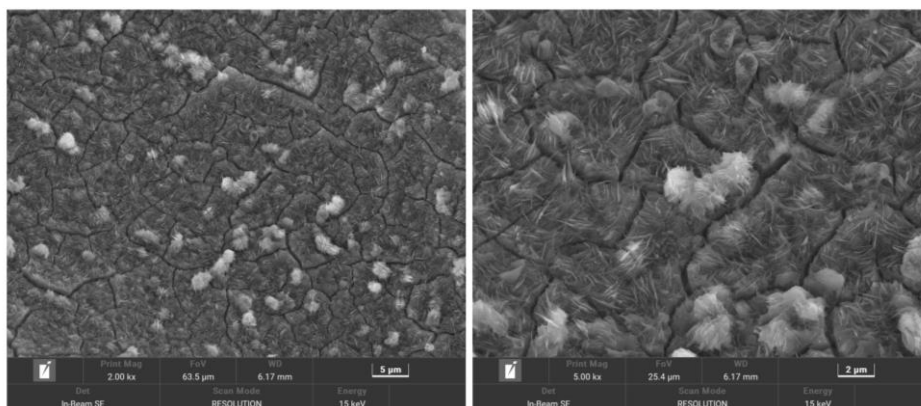


**Fig. S1** SEM images of Ru@NiFe-MOF/NF.

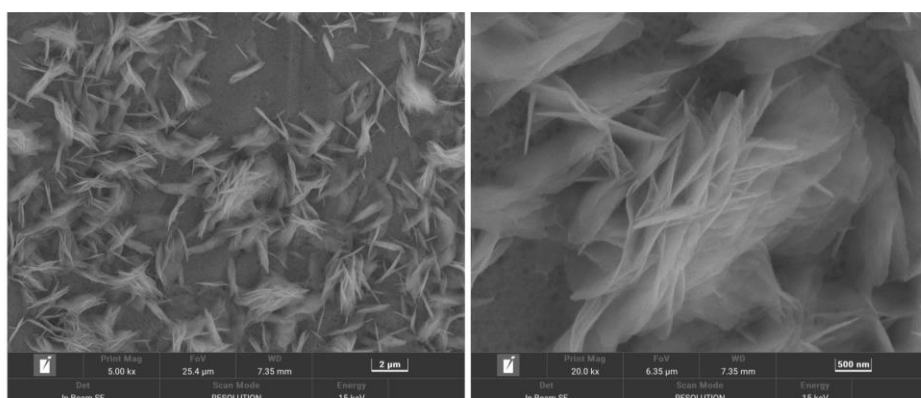


**Fig. S2** SEM images of Ru@Ni-MOF/NF.

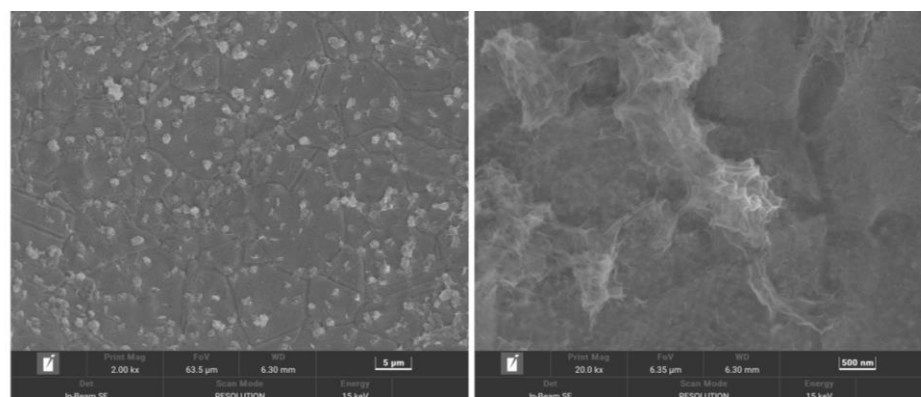


**Fig. S3** SEM images of Ru@Fe-MOF/NF.

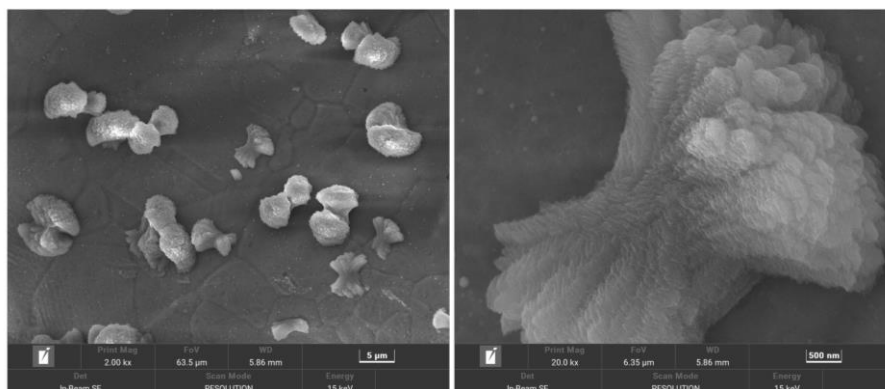


**Fig. S4** SEM images of Ru@NiCo-MOF/NF.

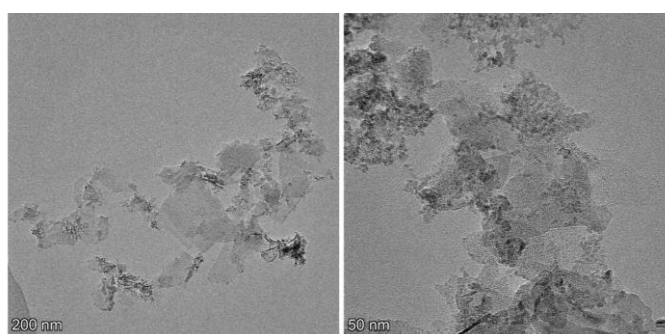


**Fig. S5** TEM images of Ru@NiFe-MOF/NF.

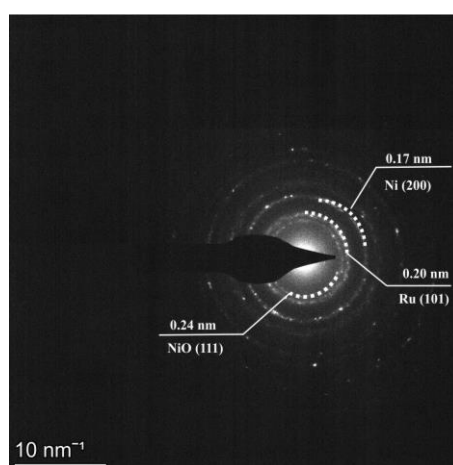


**Fig. S6** SAED pattern of Ru@NiFe-MOF/NF.

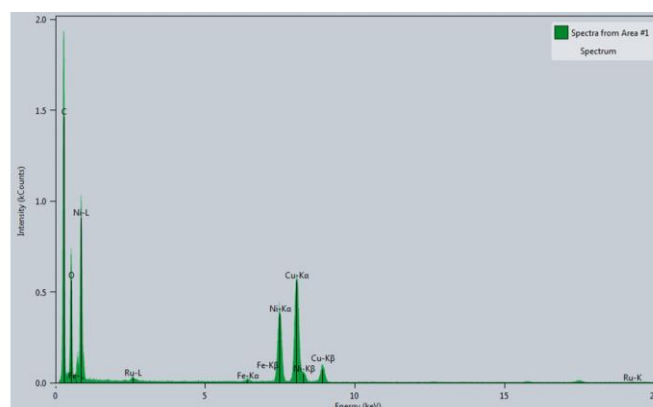


**Fig. S7** EDS spectrum of Ru@NiFe-MOF/NF.

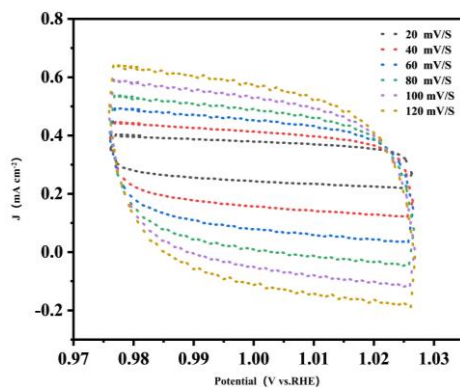


**Fig. S8** CV curves of Ru@Ni-MOF/NF.

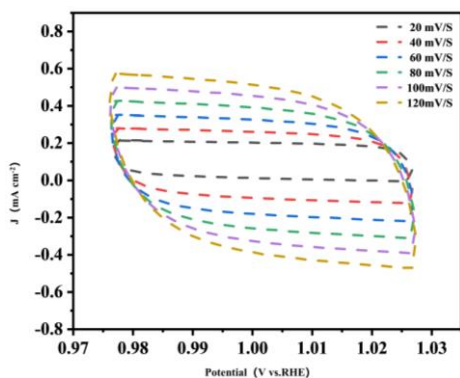


**Fig. S9** CV curves of Ru@Fe-MOF/NF.

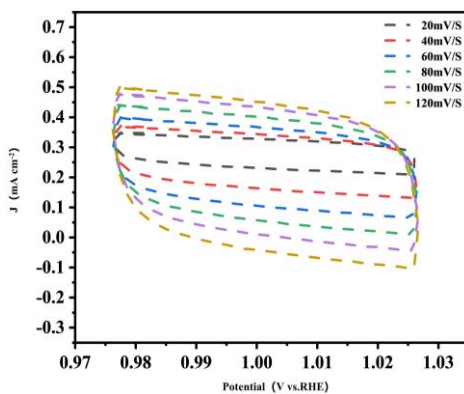


**Fig. S10** CV curves of Ru@NiFe-MOF/NF.

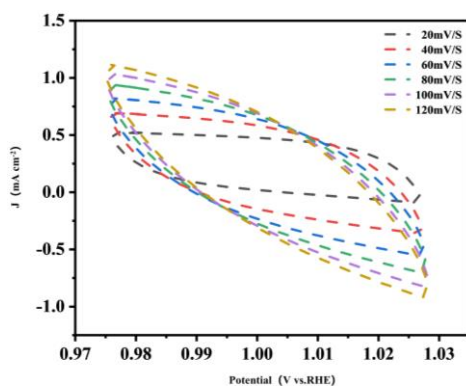


**Fig. S11** CV curves of Ru@NiCo-MOF/NF.

**Table S1** Contents of elements in the Ru@NiFe-MOFs/NF catalyst based on EDS analysis

Element	Atomic fraction/%	Mass fraction/%
C	75.48	54.29
O	16.08	15.40
Fe	0.24	0.81
Ni	7.94	27.90
Ru	0.26	1.60

**Table S2** Contents of elements in the Ru@NiFe-MOFs/NF catalyst based on XPS analysis

Element	Chemical composition/at. %
C	76.91
O	0.73
Fe	2.43
Ni	18.79
Ru	1.14

**Table S3** The content of Ru element in Ru@NiFe-MOFs/NF determined by ICP-OES

Element	Elemental content of the sample W/%
Ru	0.03